A Deterministic Chaos-Model-Based Gaussian Noise Generator

electronics

MDPI

Article

A Deterministic Chaos-Model-Based Gaussian Noise Generator

Serhii Haliuk [1], Dmytro Vovchuk [2,*], Elisabetta Spinazzola [3], Jacopo Secco [3], Vjaceslavs Bobrovs [2] and Fernando Corinto [3]

[1] Department of Radioengineering and Information Security, Yuriy Fedkovych Chernivtsi National University, 58002 Chernivtsi, Ukraine; s.haliuk@chnu.edu.ua
[2] Institute of Telecommunications, Riga Technical University, 1048 Riga, Latvia; vjaceslavs.bobrovs@rtu.lv
[3] Department of Electronics and Telecommunications, Politecnico di Torino, 10129 Torino, Italy; elisabetta.spinazzola@polito.it (E.S.); jacopo.secco@polito.it (J.S.); fernando.corinto@polito.it (F.C.)
* Correspondence: dimavovchuk@gmail.com

Abstract: The abilities of quantitative description of noise are restricted due to its origin, and only statistical and spectral analysis methods can be applied, while an exact time evolution cannot be defined or predicted. This emphasizes the challenges faced in many applications, including communication systems, where noise can play, on the one hand, a vital role in impacting the signal-to-noise ratio, but possesses, on the other hand, unique properties such as an infinite entropy (infinite information capacity), an exponentially decaying correlation function, and so on. Despite the deterministic nature of chaotic systems, the predictability of chaotic signals is limited for a short time window, putting them close to random noise. In this article, we propose and experimentally verify an approach to achieve Gaussian-distributed chaotic signals by processing the outputs of chaotic systems. The mathematical criterion on which the main idea of this study is based on is the central limit theorem, which states that the sum of a large number of independent random variables with similar variances approaches a Gaussian distribution. This study involves more than 40 mostly three-dimensional continuous-time chaotic systems (Chua's, Lorenz's, Sprott's, memristor-based, etc.), whose output signals are analyzed according to criteria that encompass the probability density functions of the chaotic signal itself, its envelope, and its phase and statistical and entropy-based metrics such as skewness, kurtosis, and entropy power. We found that two chaotic signals of Chua's and Lorenz's systems exhibited superior performance across the chosen metrics. Furthermore, our focus extended to determining the minimum number of independent chaotic signals necessary to yield a Gaussian-distributed combined signal. Thus, a statistical-characteristic-based algorithm, which includes a series of tests, was developed for a Gaussian-like signal assessment. Following the algorithm, the analytic and experimental results indicate that the sum of at least three non-Gaussian chaotic signals closely approximates a Gaussian distribution. This allows for the generation of reproducible Gaussian-distributed deterministic chaos by modeling simple chaotic systems.

Keywords: chaotic models; chaotic circuits; Gaussian noise; central limit theorem

Citation: Haliuk, S.; Vovchuk, D.; Spinazzola, E.; Secco, J.; Bobrovs, V.; Corinto, F. A Deterministic Chaos-Model-Based Gaussian Noise Generator. *Electronics* **2024**, *13*, 1387. https://doi.org/10.3390/electronics13071387

Academic Editor: Costas Psychalinos

Received: 3 March 2024
Revised: 31 March 2024
Accepted: 1 April 2024
Published: 6 April 2024

1. Introduction

Chaos theory has radically revolutionized our understanding of the potential for complex, unpredictable behavior within seemingly simple deterministic systems. This phenomenon, known as chaos, arises in nonlinear systems and is characterized by extreme sensitivity to initial conditions, often leading to the iconic "butterfly effect". Chaotic dynamics are remarkably pervasive, manifesting in diverse domains such as social, biological, and technical systems [1–6].

Security threads and challenges prompt scientists to research how chaotic signals are suitable to resolve these issues. Numerous applications have been proposed, including

secure and covert communication, pseudo-random number generators (PRNGs) and cryptography [7–14]. Despite the diverse applications and varying advantages and drawbacks in each of these scopes, chaotic systems are used as sources of entropy, a fundamental property crucial for security applications.

Chaos generators, present in both hardware and software implementation, produce time series that either mask information-bearing signals or undergo postprocessing for various cryptographic purposes. Chaotic trajectories form strange attractors in phase space, which, in contradiction to the limit cycle that represents regular behavior, have fractional or fractal dimensions [1]. There are several variants of fractal dimensions, generally measuring the average closeness, density, and distribution of points on chaotic attractors in phase space. Chaos sources are categorized into two groups, including continuous time and discrete map systems. Due to differences in attractor properties, the trajectories of a chaotic system exhibit different statistics reflected in their probability density functions (PDFs). Chaos applications necessitate a high-quality entropy source, emphasizing the necessity to maximize the entropy of chaotic signals. Statistical analyses have been proposed by Yong Wang et al. to increase the quality of chaos for the same purpose as in this paper [15]. Concerning PDFs, the most important are a number with a uniform PDF and Gaussian-distributed signals with a bell-shaped PDF. The first requirement is common in cryptography; the second is useful in communication. Both of them maximize the uncertainty of range-limited and variance-limited signals, respectively [16].

A two-dimensional discrete-time white Gaussian noise generator was proposed in [17]. To obtain an independent time series with a Gaussian probability density function, a special transformation was used on the tent map. A similar approach to the same tent map demonstrated the efficiency of the transformation method [18].

A Gaussian distribution is not the sole target widely sought in signal processing. Contributions in this direction also focus on achieving a uniform probability density. In [19], it is proven that the folding sums of chaotic trajectories, bounded within a given interval by modulus operation, tend to approach uniformity. It is worth noting that certain discrete chaotic systems yield series with a uniform probability density function without requirement of additional transformations [20–25].

Significant achievements have been attained in the realm of optical chaos generators [26–31]. Wideband optical chaos exhibits a heightened propensity for Gaussian-distributed probability density functions. This characteristic has prompted suggestions for harnessing optical chaos generators as high-quality, ultra-fast entropy sources [28,29]. A recently reported experimental technique focuses on generating a Gaussian-invariant distribution [32]. Such sources hold potential for diverse applications spanning communication [33,34], random number generation [26,27], and cryptography [30,35].

Covert communication, originally designed to conceal and render the transmission undetectable, is now being harnessed for commercial and private applications to provide physical-level protection. In contrast to conventional communication, where Gaussian white noise diminishes the signal-to-noise ratio, covert communication employs it as a countermeasure against eavesdroppers. Thermal noise is utilized to randomize the transmitted signal in a Gaussian-distributed spread spectrum [36]. Additionally, extending this concept, the utilization of artificially generated Gaussian-distributed noise has been proposed across diverse scenarios [37–40]. Despite the fact that hundreds of chaotic systems have been designed and studied, few of them can produce Gaussian-distributed signals. Therefore, finding an approach for obtaining the most complex chaotic signal based on simple and well-studied nonlinear systems is important. In this paper, we propose a method to obtain Gaussian-distributed signals. To achieve this, we study the statistical properties of some chaotic signals to find out how much of them are necessary to form a Gaussian-distributed waveform with the following experimental investigation and achievement verification that allow for an implementation of "deterministic noise" generators. With this aim, we have suggested an algorithm that combines the most valued statistical characteristics for the considered signal assessment.

The manuscript is organized as follows. In Section 2, we describe the quality metrics used to evaluate and compare chaotic signals. The properties of time series produced by mathematic models of Chua's circuit and the Lorenz system are studied in Section 3. Experimental verification of the results is provided in Section 4. The discussion and conclusion are presented in Section 5. Appendix A presents the results of computing the statistical properties of more than 40 continuous-time chaotic systems found in the literature.

2. Materials and Methods

2.1. Central Limit Theorem

The central limit theorem (CLT) relates to probability theory and explains why Gaussian noise is widespread in nature. For identically distributed independent samples, the standardized sample mean tends towards the standard normal distribution even if the original variables themselves are not normally distributed. There are several variants of the CLT. In its common Lindeberg–Lévy form, the CLT is as follows [41,42]:

Theorem 1. *Suppose* $\{X_1, \ldots, X_n\}$ *is a sequence of independent and identically distributed random variables with expectation* $\mathbb{E}[X_i] = \mu$ *and variance* $\mathrm{Var}[X_i] = \sigma^2 < \infty$*. Then, as n approaches infinity, the random variables* $\sqrt{n}(\frac{1}{n}\sum_{i=1}^{n} X_i - \mu)$ *converge in distribution to a normal* $\mathcal{N}(0, \sigma^2)$*.*

The CLT shows a way to obtain a variable with a Gaussian-like distribution from several others by summation. The key condition for particular components is their limited variance, which chaotic signals satisfy due to the existence of their attractors in bounded phase space. The question is to find how many independent chaotic signals are necessary and which criteria the resulting signal should meet to be considered Gaussian-like. Therefore, the following consideration of the basic distributions will present the possibility to develop an algorithm for testing chaotic signals.

2.2. Basic Distributions

As a reference signal, we chose white Gaussian noise whose statistical properties can be described by three basic distributions which are the PDF of the shape, the envelope and the phase of the signal.

The term "Gaussian noise" or "Gaussian signal" refers to a normal or bell-shaped probability density function of a signal. Such signals can be either random noise or information-bearing. A Gaussian variable has the following PDF

$$p(x) = \frac{1}{\sqrt{2\pi}\sigma} e^{-\frac{(x-\mu)^2}{2\sigma^2}}, \tag{1}$$

where σ—standard deviation; μ—mathematical expectation or mean.

The envelope of white noise has a Rayleigh distribution

$$p(x, \sigma) = \frac{x}{\sigma^2} e^{-\frac{x^2}{2\sigma^2}}, \tag{2}$$

where σ—standard deviation of the Gaussian distribution (1).

A uniform distribution describes the phase of a signal

$$p(\phi) = \frac{1}{2\pi}, \tag{3}$$

where $0 \leq \phi \leq 2\pi$.

2.3. Measures of Similarity of Probability Density Functions

To evaluate the similarity of any signal to WGN, normality tests that include computing of skewness and excess kurtosis are conventionally utilized [43].

Skewness is a measure of the asymmetry of a PDF around its mean and is defined as the normalized third central moment of a signal

$$\tilde{\mu}_3 = \mathbb{E}\left[\left(\frac{x-\mu}{\sigma}\right)^3\right], \tag{4}$$

where $\mathbb{E}$—expectation operator.

Excess kurtosis is the metric of the height and sharpness of a PDF relative to that of a standard bell curve

$$\tilde{\mu}_4 = \mathbb{E}\left[\left(\frac{x-\mu}{\sigma}\right)^4\right] - 3. \tag{5}$$

For WGN, both the skewness and excess kurtosis are equal to zero.

It is worth noting that if a signal exhibits a symmetric distribution with zero excess kurtosis, it by no means guarantees that its probability density function is normal. There are non-Gaussian distributions with $\tilde{\mu}_3 = 0$ and $\tilde{\mu}_4 = 0$ [44,45]. Therefore, at least a graphical analysis is necessary to confidently assert the normality of the distribution, or confirmation should be achieved through more sophisticated tests.

The envelope and phase of a signal can be found by using the Hilbert transform [46]. For a given function $x(t)$, the Hilbert transform is given as

$$\hat{x}(t) = \mathbb{H}(x(t)) = \frac{1}{\pi}\int_{-\infty}^{\infty}\frac{x(t)}{t-\tau}d\tau. \tag{6}$$

Then, the envelope and phase of $x(t)$ are

$$a(t) = \sqrt{x^2(t) + \hat{x}^2(t)}, \tag{7}$$

$$\phi(t) = \arctan\frac{\hat{x}(t)}{x(t)}. \tag{8}$$

If $x(t)$ is WGN, the envelope $a(t)$ has a Rayleigh PDF (2), and the phase $\phi(t)$ has a uniform PDF (3).

The informational properties of signals can be assessed by their differential entropy. For a variable x with a probability density function $p(x)$, the differential entropy is given by

$$h = -\int_{-\infty}^{\infty} p(x)\log p(x)dx. \tag{9}$$

The Gaussian distribution (1) attains the maximum differential entropy, which, for $\mu = 0$ and variance σ^2, is equal to

$$h_g = \frac{1}{2}\ln 2\pi e\sigma^2. \tag{10}$$

For any other signal with the same variance σ^2, the differential entropy $h(x)$ does not exceed the value given in (10), i.e., $h(x) \leq h_g(x)$.

Entropy power, a concept pioneered by Shannon [47], allows us to compare the probability density functions of a signal and Gaussian noise:

$$k_1 = \frac{e^{2h}}{2\pi e},\ 0 \leq k_1 \leq 1, \tag{11}$$

where h—entropy of signal.

The entropy power of a distribution coincides with the variance of a Gaussian distribution possessing an identical entropy.

To compare two arbitrary PDFs, we used the entropy power ratio, mathematically defined as follows for distributions $p_1(x)$ and $p_2(x)$ bearing entropies h_1 and h_2, respectively:

$$\frac{k_1(h_2)}{k_1(h_1)} = e^{2\Delta h}, \tag{12}$$

where $\Delta h = h_1 - h_2$—the difference between differential entropies of two distributions.

To restrict the value of ratio (12) into interval $0 \leq k_1 \leq 1$, the following expression can be applied:

$$k = e^{-2|\Delta h|}. \tag{13}$$

The entropy power (13) increases when the difference between entropies of distributions becomes smaller.

To evaluate the similarity of probability density functions with an amplitude and a phase with the reference distributions, we utilize the entropy power relative to these baseline distributions. Thus, the entropy power of the envelope of the signal is determined as:

$$k_2 = e^{-2|h_e - h_R|}, \tag{14}$$

where h_e—entropy of the envelope of signal; $h_R = 1 + \ln \frac{\sigma}{\sqrt{2}} + \frac{\gamma}{2}$—entropy of a Rayleigh PDF (2) [44]; and $\gamma \approx 0.577$—Euler–Mascheroni constant.

The entropy power for evaluating the similarity of the phase distribution of the signal and a uniform one would be determined as:

$$k_3 = e^{-2|h_{ph} - h_u|}, \tag{15}$$

where h_{ph}—entropy of the phase of the signal; $h_u = \ln 2\pi$—entropy of a uniform PDF (3) [44].

Furthermore, the cross-entropy and Kullback–Leibler divergence can serve as additional metrics within the considered algorithm [48]. While not explicitly highlighted in the text, their analysis has been performed preliminarily, revealing clear results that they do not hold a decisive role in characteristic assessments for this type of study.

3. Properties of Sums of Chaotic Signals

The approach for generating a Gaussian-distributed chaotic signal is schematically illustrated in Figure 1. Selected chaotic outputs undergo normalization, followed by summation, to achieve a transformation from their original probability density function to a Gaussian PDF. The normalization step may be omitted depending on the properties of the original chaotic signals and the desired variance of the resulting sum.

There are lots of different nonlinear systems exhibiting chaotic behavior. We investigated more than 40 mostly three-dimensional chaotic systems through computing the PDFs, skewness, excess kurtosis, and entropy power of their output signals. Before estimation of the characteristic mentioned in the algorithm, each chaotic signal was centered around its zero mean and normalized to have unit variance. The results show that the majority of the studied chaotic systems exhibit characteristics that are far from being considered Gaussian-like signals.

The obtained results for a variety of chaotic systems appear in Appendix A, and a detailed description of the algorithm is analytically and experimentally demonstrated below with examples from two widely used and extensively studied systems: Chua and Lorenz. They were specifically chosen since their signals, among all examined, possess the most favorable parameters to serve as a platform for generating deterministic chaotic Gaussian signals.

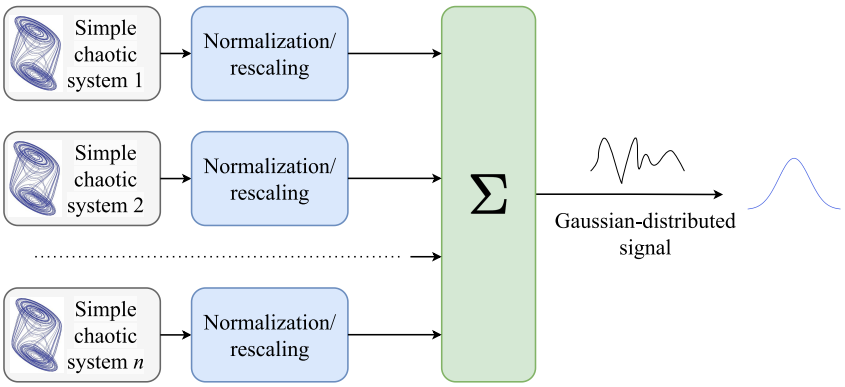

Figure 1. Schematic representation of the suggested algorithm for forming Gaussian-distributed signals. Simple chaotic systems with different initial conditions and/or system parameters suffer normalization (an optional stage depending on the conditions) and are added in the summation block. The number of chaotic systems (n) can vary until the output signal successfully passes the suggested algorithm's tests, resulting in the achievement of a Gaussian-distributed signal.

3.1. Chua's Circuit

Chua's circuit is one of the most well-known systems that generate deterministic chaos and can be easily implemented as an electrical circuit [49]. Moreover, various types of nonlinearities can be utilized in this circuit [50,51].

The mathematical model of Chua's circuit in dimensionless form is a three-differential equation system

$$\begin{aligned} \dot{x} &= \alpha(y - x - f(x)) \\ \dot{y} &= x - y + z \\ \dot{z} &= -\beta y \end{aligned} \tag{16}$$

where x, y, z—output variables; α, β—parameters of the model; and $f(x) = m_2 x + 0.5((m_0 - m_1)(|x + a_1| - |x - a_1|) + (m_1 - m_2)(|x + a_2| - |x - a_2|))$—nonlinear function, where $a_1 = 1$, $a_2 = 6.88$, $m_0 = -1.238$, $m_1 = -0.6665$, $m_2 = 500$. The connection between the circuit's and the model's parameters can be found in [49,52].

A key requirement to obtain independent chaotic systems is the absence of any connection between them. In analytical analysis, the independence of chaotic systems is achieved through different initial conditions of the systems; in experiments, it occurs due to the difference between the system parameters and the initial conditions, which appears naturally.

We studied Chua's circuit with a piecewise linear characteristic in the nonlinear part, which provides various dynamical modes, including a single- or double-scroll chaotic attractor. As shown in Figure 2, the circuit consists of inductance, two capacitors, and nonlinearity and is implemented on two operational amplifiers [52].

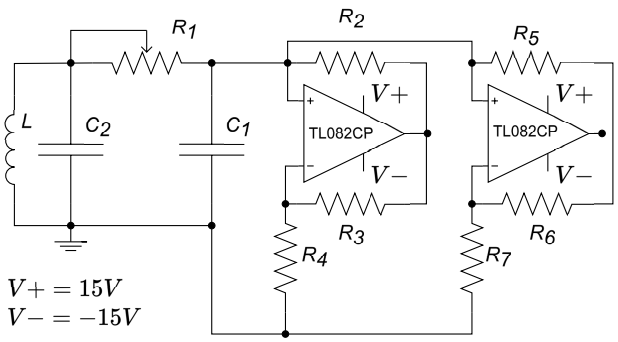

Figure 2. Chua's circuit.

When $\alpha = 10$ and $\beta = 14.6$, the circuit operates in double-scroll mode and all the outputs possess a symmetric PDF with skewness close to zero. The y output produces a low excess kurtosis $\tilde{\mu}_4 = 0.1421$, which also has the highest entropy power of $k_1 = 0.9039$, $k_2 = 0.9756$, and $k_3 = 0.998$. Nevertheless, there are distinct visual differences between the PDFs of chaotic and basic distributions, which can be seen in Figure 3a,e,i and numerically from Table A1.

The central limit theorem states that the summation of two or more chaotic signals yields a PDF of the sum that exhibits a greater resemblance to a Gaussian PDF compared to that of a single signal. The evolution of the PDFs when the number n of independent chaotic signals increases is shown in Figure 3. To minimize the number of chaotic signal in the total signal, it is efficient to use the variable y. When only three independent outputs of y are added, the PDF of the sum, along with its envelope and phase, closely resembles the basic PDFs, i.e., normal, Rayleigh, and uniform PDFs. The entropy powers of the sum k_1, k_2, k_3 exceed 0.99.

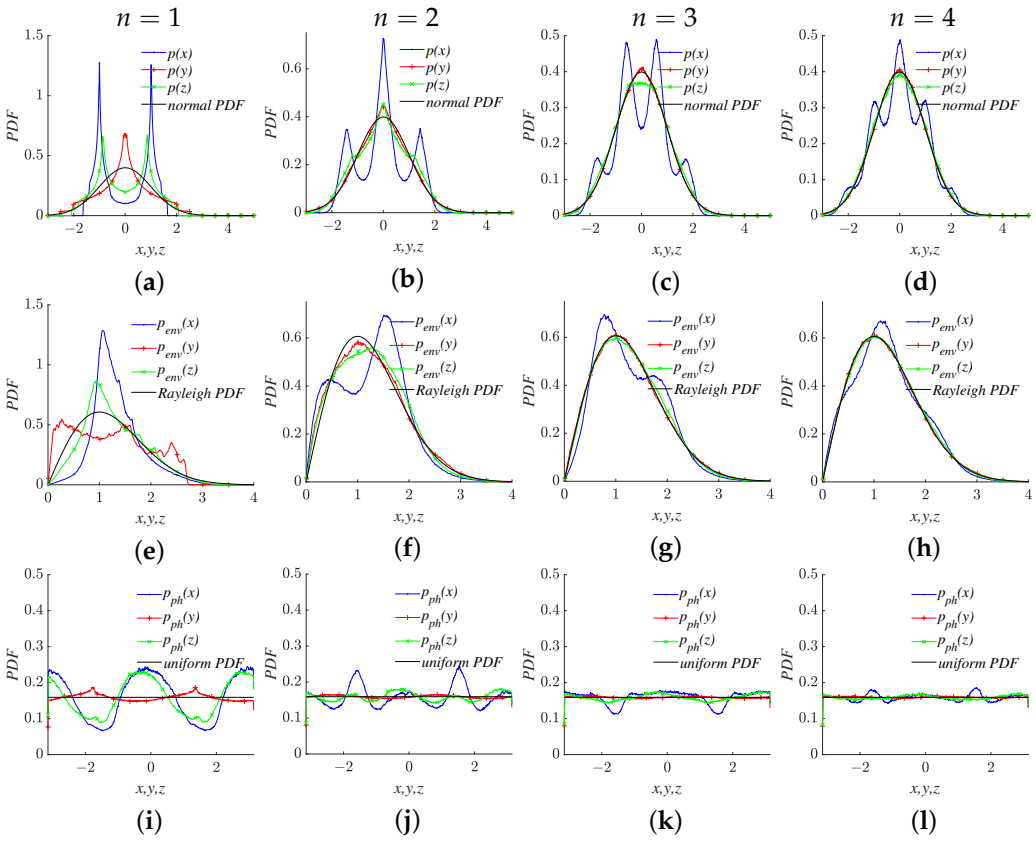

Figure 3. The PDFs of the sum of n chaotic signals generated by Chua's circuit: PDF of signals (**a**–**d**), PDF of envelope of signals (**e**–**h**), PDF of the phase of signals (**i**–**l**).

The quality metrics of the sum of signals are contingent upon the number of signals incorporated, as illustrated in Figure 4. The excess kurtosis decreases to zero, and all entropy powers converge to 1 with an increasing value of n. This suggests that achieving chaos resembling Gaussian noise necessitates the addition of a minimum of three original chaotic signals from Chua's circuit.

A change in circuit parameters with preservation of the chaotic double-scroll mode causes significant changes in the quality metrics, particularly the excess kurtosis and entropy power. For example, when $\alpha = 9.273$ and $\beta = 16.8$, Chua's circuit has the following metrics, which are quite different from ones mentioned above: $E = -0.9334$, $k_1 = 0.8739$, $k_2 = 0.5006$ and $k_3 = 0.999$. This result suggests that the PDFs of signals are sensitive to the parameters of the chaotic system.

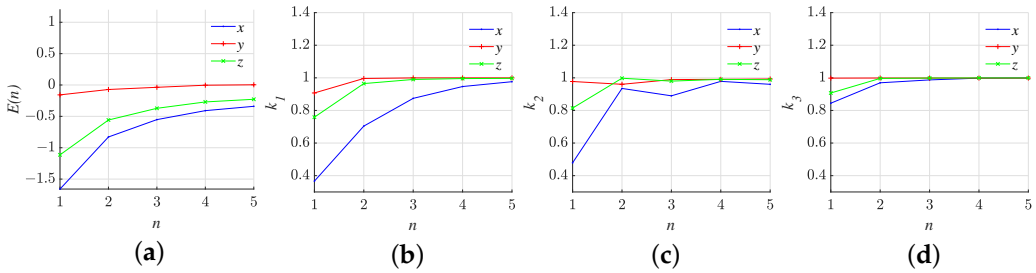

Figure 4. Quality metrics of the sum of n signals x, z generated by Chua's circuit for different n: excess kurtosis (**a**), entropy power of the amplitude of signals (**b**), entropy power of the envelope of signals (**c**) and entropy power of the phase of signals (**d**).

3.2. Lorenz System

While the previously considered Chua's circuit is one of the simplest both as an analytical model and an experimental implementation, the Lorenz system is a well-known and extensively investigated source of deterministic chaos. The system was originally developed to model atmospheric convection in meteorology and allows for the description of different atmospheric phenomena [53]. The Lorenz system is usually applicable in its mathematical representation (a system of three differential equations with nonlinearity (17)) and has found widespread use in diverse fields such as physics, engineering, biology, economics, and even art. However, its hardware implementation is inherently more complex than Chua's circuit due to the involvement of analog multipliers (Figure 5) [54].

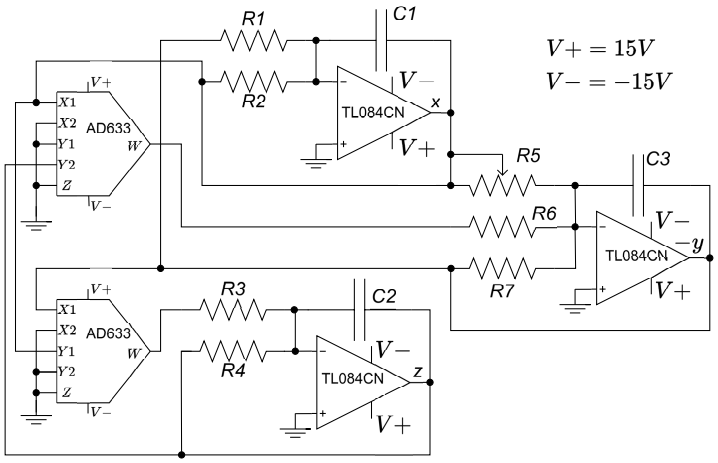

Figure 5. Electronic implementation of a Lorenz system.

$$\begin{aligned} \dot{x} &= \sigma(y - x) \\ \dot{y} &= (r - z)x - y \\ \dot{z} &= xy - bz \end{aligned} \tag{17}$$

where x, y, z—system variables; $\sigma = 10$, $r = 28$, and $b = \frac{8}{3}$—parameters.

We simulated system (17) with two different values of the parameter r, $r = 28$ and $r = 60$, keeping other parameters constant. The statistic parameters of the Lorenz system are shown in Table A2. Two of the three outputs in the Lorenz system, namely x and y, exhibit symmetric PDFs. Similarly to Chua's circuit, the results indicate a significant impact of the model parameters on the appearance and characteristics of the PDFs of the output signals. For the investigated parameter values, the signal most resembling Gaussian noise is y, with $\sigma = 10$, $r = 28$, and $b = \frac{8}{3}$, featuring coefficients $\tilde{\mu}_4 = -0.1573$, $k_1 = 0.9013$, $k_2 = 0.9368$, and $k_3 = 0.8877$.

The original histograms of normalized output signals from the Lorenz system are shown in Figure 6. Despite the asymmetry in the output signal z, combining all three

outputs can yield a normal PDF when summing only three–four signals. The relationship between the excess kurtosis coefficient and entropy powers for different values of n is presented in Figure 7 and confirms this conclusion.

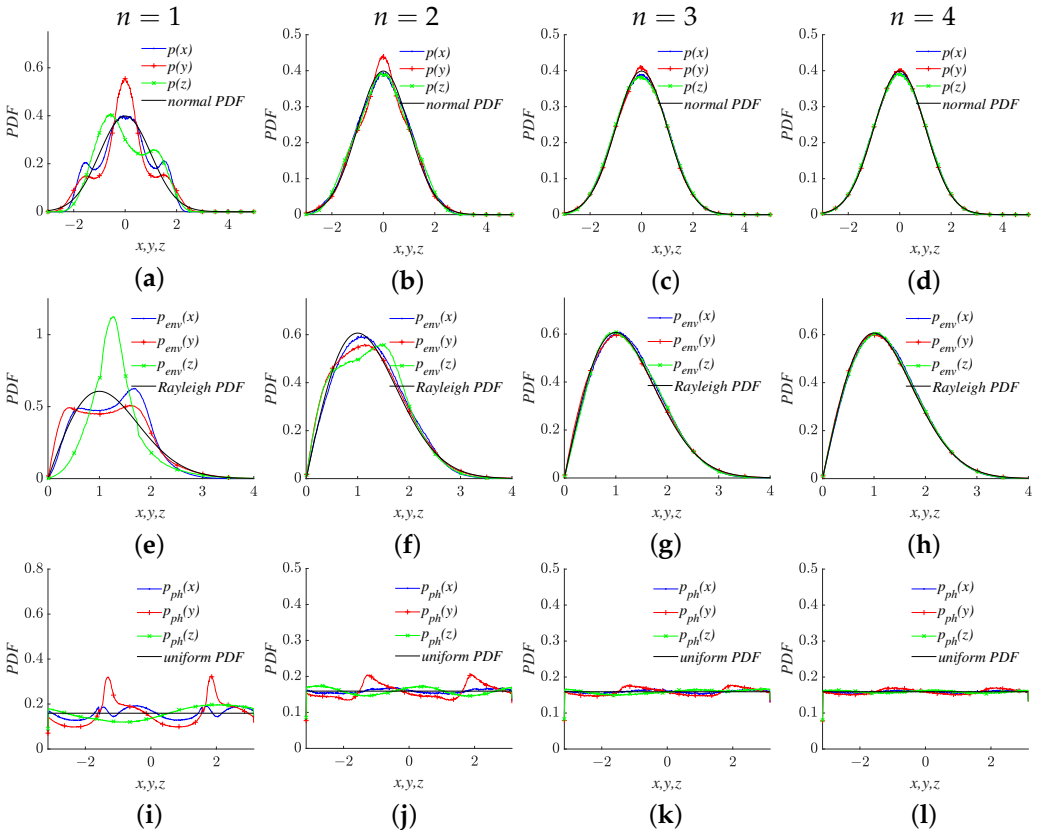

Figure 6. The PDFs of the sum of n chaotic signals generated by a Lorenz circuit: PDF of signals (**a**–**d**), PDF of envelope of signals (**e**–**h**), PDF of the phase of signals (**i**–**l**).

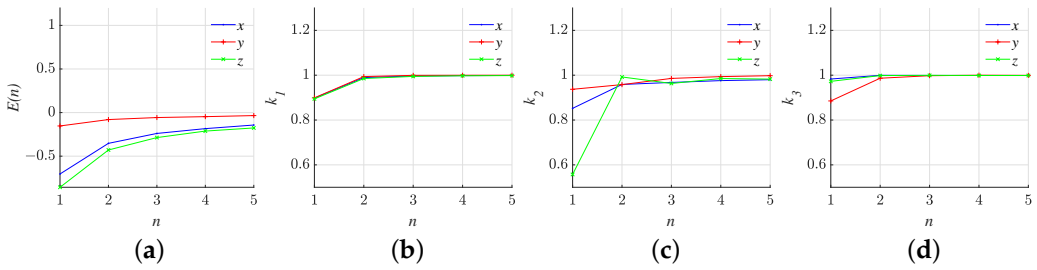

Figure 7. Quality metrics of the sum of n signals x, y, and z generated by a Lorenz circuit for different n: excess kurtosis (**a**), entropy power of the amplitude of signals (**b**), entropy power of the envelope of signals (**c**) and entropy power of the phase of signals (**d**).

The entropy power values (k_1, k_2, k_3) for the sum of three and four y variables exceed 0.98 and 0.99, respectively. Furthermore, a comparison of the PDFs in Figure when $n = 4$ suggests there are no significant discrepancies between the PDFs of the sum and the basic PDFs.

Analyses of Chua's circuit and the Lorenz system reveal that the summation of chaotic non-Gaussian signals proves to be an effective method for obtaining deterministic chaotic Gaussian signals.

4. Experimental Verification

4.1. Experiment with Chua's Circuit

The following results were obtained for the Chua circuit with a piecewise linear–nonlinear element implemented using TL082CP operational amplifiers, as depicted in Figure 2. Four circuits were assembled with slightly different parameters. The parameter difference was determined by the used components' features—for the used capacitors, $C1 = 100$ µF and $C2 = 10$ µF; for the inductor, $L = 18$ mH; and they both have a tolerance of ±5%. The parameters of the nonlinear element were as $R2$, $R3 = 220$ Ohm, $R4 = 2.2$ kOhm, $R5$, $R6 = 22$ kOhm, and $R7 = 3.3$ kOhm.

Additionally, a potentiometer was utilized to provide a resistance $R1 = 1580$ Ohm, the value of which could be adjusted in increments of ±100 Ohm to change the chaotic circuit behavior. The voltages across the capacitors C_2, corresponding to the variable y in the model of the circuit, were recorded and processed for further analysis. A set of signal records (50 samples of voltages across the capacitors C_2) was obtained, where each record contained 2×10^6 sweep points.

The experimental results confirmed the theoretical assumptions and analytical outcomes. As depicted in Figure 8, increasing the number of chaotic systems rapidly drives the distribution of their summed signals towards a normal distribution. This observation extends to the envelope and phase of the signal, where Rayleigh and uniform distributions were observed, respectively.

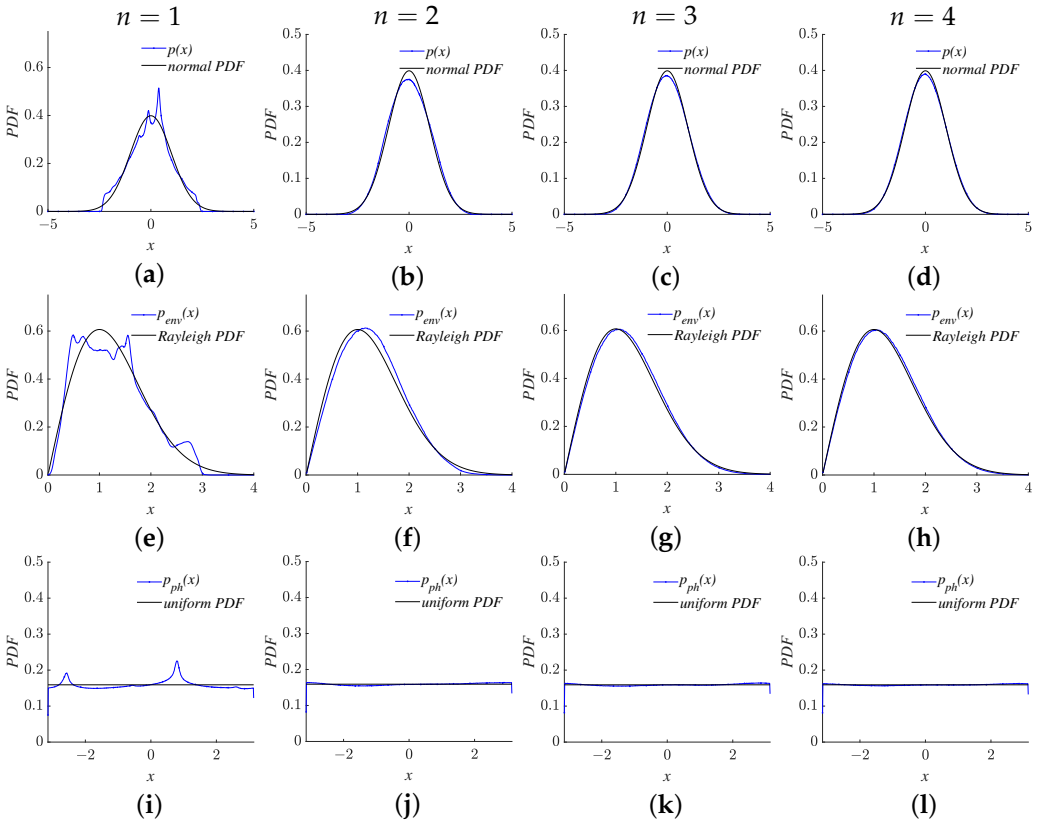

Figure 8. The experimental PDFs of the sum of n chaotic signals generated by a prototype of Chua's circuit: PDF of signals (**a**–**d**), PDF of envelope of signals (**e**–**h**), PDF of the phase of signals (**i**–**l**).

4.2. Experiment with a Lorenz System

An experimental investigation was performed using a simplified electronic realization of a Lorenz oscillator, constructed in accordance with the specifications outlined in [54,55] and the circuit in Figure 5. We used an AD633 analog multiplier and a TL084CN operational amplifier. The other circuit elements were as follows: $R1, R2 = 100$ kOhm, $R3$, $R6 = 10$ kOhm, and $R7 = 1$ MOhm, with a tolerance of 5%, and $R4 = 370$ Ohm, with a

tolerance of 0.5%. The variable resistor $R5$ allows for tuning of the parameter r and was set at $R5 = 35.72$ kOhm.

Four circuits were assembled on a breadboard, and the appropriate oscillograms were recorded. Subsequently, they were subjected to the suggested set of tests. The probability density functions of the normalized output x from the electronic circuit of the Lorenz system are illustrated in Figure 9. A comparison between Figures 9 and 6 reveals a good agreement between the analytic and experimental results.

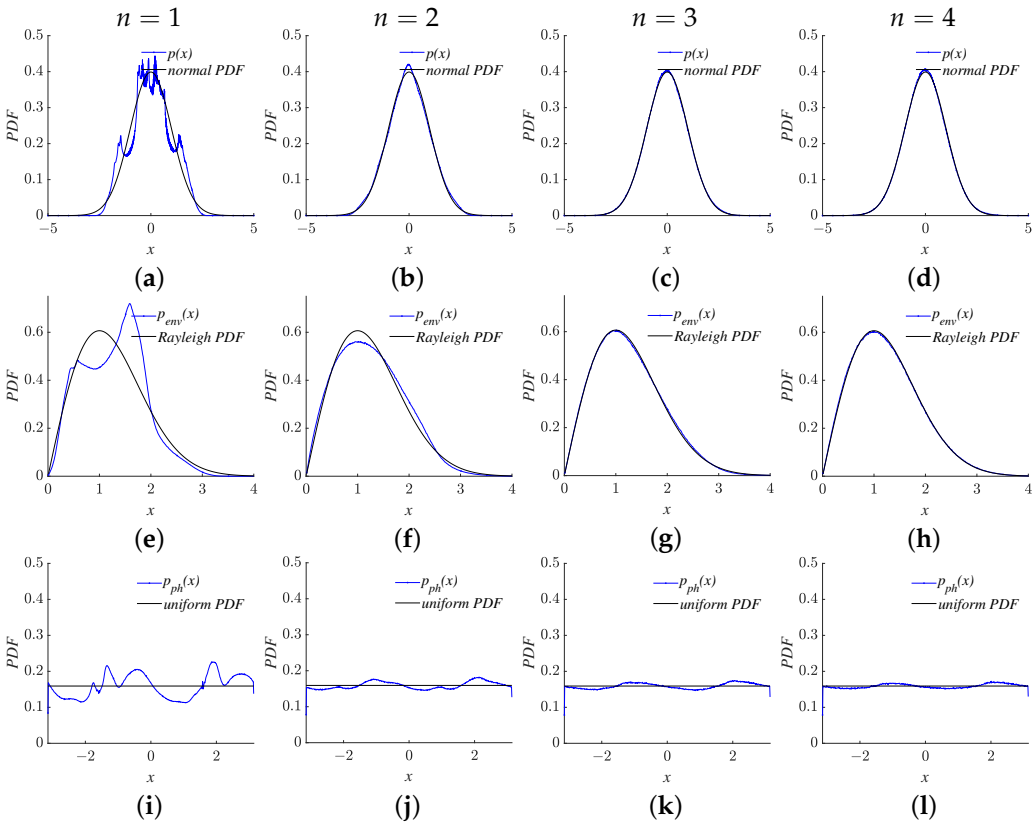

Figure 9. The experimental PDFs of the sum of n chaotic signals generated by a prototype of a Lorenz circuit: PDF of signals (**a**–**d**), PDF of envelope of signals (**e**–**h**), PDF of the phase of signals (**i**–**l**).

5. Discussion and Conclusions

The results underscore a promising approach for generating deterministic Gaussian-like signals using an optimal number of chaotic systems. The PDFs of the original chaotic signals exhibit essential deviations from a normal distribution, indicating their inherently lower information capacity compared to fully random Gaussian noise. This observation prompts the need to establish criteria for selecting chaotic systems to achieve Gaussian signal formation through the summation of chaotic signals. This requires an optimization process to minimize the number of independent simple chaotic signals. The performed analysis demonstrates that adherence to the following guidelines significantly enhances the likelihood of a successful chaotic system and signal selection:

i. Prioritize signals possessing symmetric probability density functions.
ii. Minimize the excess kurtosis of the selected signals, ideally aiming for $\tilde{\mu}_4 < 1$.
iii. Ensure that all three entropy powers (k_1, k_2, k_3) of the original chaotic signal surpass a value of 0.85.

While strict adherence to these guidelines does not ensure Gaussian signal achievement, it substantially increases the probability of generating a Gaussian chaotic signal with the desired entropy coefficients $k_1, k_2, k_3 > 0.95$. Although, theoretically, there are no limitations to the number of chaotic signals that can be summed to achieve a Gaussian dis-

tribution, practical implementation has restrictions due to the lack and value of resources and the size limitation of devices. The lowest limit is defined by using the algorithm considered in this paper to merely sum three or four independent chaotic signals.

It is crucial to underscore that chaotic signals are generated by deterministic systems, rendering their summation equally deterministic. This underscores the capability of simple summation to yield intricate, noise-mimicking chaotic signals that retain their deterministic nature. The most innovative aspect of this method is the possibility of attributing the output voltage and the current of random chaotic circuits of a well-known signal as Gaussian noise, the properties of which are well known and exploitable in many applications. The possibility of obtaining a Gaussian-like signal description presents the opportunity to design and model chaotic circuits' output voltages, preserving all the general properties of the Gaussian distribution. Moreover, since many chaotic circuits do not have output signals linked to Gaussian noise, this method allows for widening the field of investigation, even to those circuits that apparently do not have these properties. It is also considerable that more than 40 chaotic systems have been evaluated, leading to the confirmation of this theory and confirming the validity of this method.

The output signals obtained via this process hold considerable value across a variety of applications, including generating deterministic Gaussian noise, electronic warfare systems, coherent and/or covert communication systems, radars, statistical modeling, machine learning, cryptography, and more.

The possibility of obtaining a pseudo-random number generator through the simple sum of chaotic signals predisposes this method to a wide range of applications, bypassing any possible complications of chaotic signal processing. All the possible applications mentioned can support both hardware and software implementation of chaotic circuits, with the addition in this case of greater properties and guidelines that can be exploited during the implementation guaranteed by the traceability to Gaussian noise. Since the main aim is to present more known laws of circuits that in certain conditions are dominated by chaos, other aspects and elaborations of the output signals of the proposed chaotic circuits are also being investigated, which could lead back to the properties of pseudo-Gaussian noise. Future investigations will aim at trying to reconstruct more well-known properties of apparently chaotic signals, trying to make it easier to implement the chosen application.

The results of the study can find applications in the enhancement of security in communication systems. These include:

i. Covert communication—there are approaches based on thermal noise or AI noise; therefore, our recommendation is to use artificial Gaussian-distributed chaotic signals for hidden communication;
ii. Radio countermeasure purposes—the deterministic nature of chaotic systems can be used to reproduce and compensate for the influence of chaos in "friendly devices" and remains incomprehensible for "enemies". This means that the same signal can be at least neutral for one device and harmful to others;
iii. PRNG for cryptography purposes—a huge number of scientific studies are concerned with this question. By increasing the number of chaotic signals, we increase the keyspace of the encrypted information.

The Gaussian noise model serves as a foundational and widely applicable framework for analyzing signal randomness. However, it is important to recognize that while Gaussian noise is a common and versatile model, quite a few diverse noise models exist that can be useful. Examples include pink noise, brown noise, and various others, which are rather a special case of the Gaussian noise model, but require additional consideration to use them as a reference for the development of a random signal testing algorithm.

Author Contributions: Conceptualization, S.H.; methodology, S.H. and D.V.; software, S.H., E.S. and J.S.; validation, V.B. and F.C.; formal analysis, all authors; investigation, S.H., D.V., E.S. and J.S.; resources, V.B. and F.C.; data curation, S.H. and D.V.; writing and original draft preparation, all authors; visualization, all authors; supervision, V.B. and F.C.; project administration, V.B. and F.C. All authors have read and agreed to the published version of the manuscript.

Funding: This research was funded by the RRF project Latvian Quantum Technologies Initiative Nr. 2.3.1.1.i.0/1/22/I/CFLA/001.

Data Availability Statement: The data that support the findings of this study are available from the corresponding author upon reasonable request.

Conflicts of Interest: The authors declare no conflicts of interest.

Appendix A

Tables A1–A3 present the results of passing the suggested algorithm tests, including skewness $\tilde{\mu}_3$, excess kurtosis $\tilde{\mu}_4$, and entropy power for signal k_1, its envelope k_2, and phase k_3. The initial conditions for the majority of chaotic systems were randomly selected from the interval (0, 1). In cases where the chaotic mode demonstrates dependence on the initial conditions, the specific values are indicated in Table A3. Signals suitable for summation are highlighted in green, while those that successfully passed the suggested algorithm's tests are highlighted in blue.

Table A1. Statistical properties of signals of Chua's circuit.

Chaotic System	Output Variable	$\tilde{\mu}_3$	$\tilde{\mu}_4$	k_1	k_2	k_3
Chua's circuit [49]						
$\dot{x} = 10(y - x - f(x))$	x	−0.0116	−1.6609	0.3626	0.4754	0.8435
$\dot{y} = x - y + z$	y	−0.0028	−0.1421	0.9039	0.9756	0.9980
$\dot{z} = -14.6y$	z	0.0084	−1.1152	0.7541	0.8128	0.9056
where						
$f(x) = m_2x + 0.5((m_0 - m_1)(\lvert x + a_1\rvert - \lvert x - a_1\rvert) + (m_1 - m_2)(\lvert x + a_2\rvert - \lvert x - a_2\rvert))$;						
$a_1 = 1$; $a_2 = 6.88$; $m_0 = -1.238$; $m_1 = -0.6665$; $m_2 = 500$.						
Pairwise sum of two signals						
$x_1 + x_2$		0.0033	−0.8287	0.7040	0.9349	0.9696
$y_1 + y_2$		0.0029	−0.0717	0.9961	0.9604	0.9989
$z_1 + z_2$		−0.0007	−0.5581	0.9648	0.9976	0.9965
Pairwise sum of three signals						
$x_1 + x_2 + x_3$		−0.0059	−0.5519	0.8741	0.8897	0.9873
$y_1 + y_2 + y_3$		0.0015	−0.0367	0.9996	0.9893	0.9986
$z_1 + z_2 + z_3$		0.0089	−0.3715	0.9901	0.9798	0.9987
Pairwise sum of four signals						
$x_1 + x_2 + x_3 + x_4$		−0.0090	−0.4088	0.9467	0.9783	0.9982
$y_1 + y_2 + y_3 + y_4$		0.0009	−0.0034	0.9998	0.9908	0.9985
$z_1 + z_2 + z_3 + z_4$		0.0105	−0.2700	0.9955	0.9907	0.9994
Experiment with Chua's circuit						
y_1	y	−0.0518	−0.4249	0.9437	0.9381	0.9950
$y_1 + y_2$		0.0339	−0.3837	0.9897	0.9192	0.9986
$y_1 + y_2 + y_3$		0.0511	−0.2393	0.9962	0.9629	0.9986
$y_1 + y_2 + y_3 + y_4$		0.0420	−0.1846	0.9979	0.9720	0.9985
Chua's circuit [49]						
$\dot{x} = 9.273(y - x - f(x))$	x	−0.0763	−1.4807	0.5463	0.6532	0.9087
$\dot{y} = x - y + z$	y	−0.0070	−0.9334	0.8739	0.5006	0.9989
$\dot{z} = -16.8y - 0.0042z$	z	0.0465	−0.8164	0.8676	0.8860	0.9808
where						
$f(x) = m_2x + 0.5((m_0 - m_1)(\lvert x + a_1\rvert - \lvert x - a_1\rvert) + (m_1 - m_2)(\lvert x + a_2\rvert - \lvert x - a_2\rvert))$;						
$a_1 = 1$; $a_2 = 6.88$; $m_0 = -1.238$; $m_1 = -0.6665$; $m_2 = 500$.						

Table A2. Statistical properties of signals of Lorenz systems.

Chaotic System	Output Variable	$\tilde{\mu}_3$	$\tilde{\mu}_4$	k_1	k_2	k_3
Lorenz [53]						
$\dot{x} = 10(y - x)$	x	0.0003	−0.7093	0.8989	0.8535	0.9830
$\dot{y} = (28 - z)x - y$	y	0.0005	−0.1573	0.9013	0.9368	0.8877
$\dot{z} = xy - \frac{8}{3}$	z	0.2023	−0.8499	0.8974	0.5618	0.9731
Pairwise sum of two signals						
$x_1 + x_2$		−0.0102	−0.3529	0.9893	0.9587	0.9995
$y_1 + y_2$		−0.0103	−0.0801	0.9938	0.9580	0.9865
$z_1 + z_2$		0.0014	−0.4291	0.9852	0.9921	0.9983
Pairwise sum of three signals						
$x_1 + x_2 + x_3$		−0.0053	−0.2393	0.9966	0.9677	0.9989
$y_1 + y_2 + y_3$		−0.0059	−0.0570	0.9993	0.9857	0.9978
$z_1 + z_2 + z_3$		0.0397	−0.2867	0.9946	0.9631	0.9994
Pairwise sum of four signals						
$x_1 + x_2 + x_3 + x_4$		−0.0031	−0.1840	0.9981	0.9759	0.9987
$y_1 + y_2 + y_3 + y_4$		−0.0040	−0.0468	0.9997	0.9937	0.9999
$x_1 + x_2 + x_3 + x_4$		0.0002	−0.2122	0.9975	0.9852	0.9987
Experiment with Lorenz system						
x_1	x	0.0131	−0.5906	0.9292	0.8454	0.9606
$x_1 + x_2$		0.0150	−0.1978	0.9937	0.9995	0.9976
$x_1 + x_2 + x_3$		0.0204	−0.0523	0.9989	0.9996	0.9993
$x_1 + x_2 + x_3 + x_4$		0.0246	0.0499	0.9995	0.9886	0.9996
Lorenz [53]						
$\dot{x} = 10(y - x)$	x	−0.0034	−0.9328	0.8961	0.7523	0.9649
$\dot{y} = (60 - z)x - y$	y	−0.0038	−0.3519	0.9801	0.9247	0.8355
$\dot{z} = xy - \frac{8}{3}z$	z	0.0821	−0.4826	0.9736	0.7515	0.9786

Table A3. Statistical properties of signals of chaotic systems.

Chaotic System	Output Variable	$\tilde{\mu}_3$	$\tilde{\mu}_4$	k_1	k_2	k_3
Bhalekar and Gejji [56]						
$\dot{x} = -2.677x - y^2$	x	−0.4940	−0.3912	0.8739	0.5924	0.9420
$\dot{y} = 10(z - y)$	y	−0.0029	−0.2152	0.9362	0.7205	0.7675
$\dot{z} = -27.3y - z + xy$	z	−0.0029	−0.0071	0.9586	0.9157	0.6919
Chen and Lee [57]						
$\dot{x} = -yz + 5x$	x	−0.0009	−1.3013	0.7086	0.2180	0.9371
$\dot{y} = xz - 10y$	y	0.0027	−0.7711	0.9037	0.3269	0.8813
$\dot{z} = \frac{1}{3}xy - 3.8z$	z	0.4027	−0.6617	0.7847	0.5387	0.9838
Cheng et al. [58]						
$\dot{x} = y$	x	0.0042	−0.7241	0.8544	0.7317	0.9969
$\dot{y} = -0.2y -$ $(0.25x \sin x)(10 \cos 2t + 0.1)$	y	0.0002	−0.6388	0.9540	0.7494	0.9792
Colpitts chaotic oscillator [59,60]						
$\dot{x} = \frac{1}{C_1}(z - \beta f(x))$	x	−1.3378	1.5271	0.5924	0.7753	0.7510
$\dot{y} =$ $\frac{1}{C_2}(\frac{1}{R_e}(v_e - y) - z - f(x))$	y	−0.9897	0.0021	0.4836	0.6179	0.9102
$\dot{z} = \frac{1}{L}(v_{ce} - x - r_L z + y)$	z	1.0142	0.3489	0.6171	0.9408	0.8144

where $C_1 = 15 \times 10^{-9}$; $C_2 = 9.7 \times 10^{-9}$; $L = 30 \times 10^{-6}$; $v_e = 2$; $R_e = 400$; $\beta = 300$; $v_{ce} = 7$; $r_L = 40$; $f(x) = \begin{cases} 0, x \leq 0.75, \\ \frac{x - 0.75}{200}, x > 0.75. \end{cases}$.

Table A3. *Cont.*

Chaotic System	Output Variable	$\tilde{\mu}_3$	$\tilde{\mu}_4$	k_1	k_2	k_3
Dong et al. [61], $[x_0, y_0, z_0] = [0.78, 0.52, 0.30]$						
$\dot{x} = a_1 x - a_2 x^2 - a_3(y+z)$	x	1.3143	15.2455	0.1413	0.2982	0.7632
$\dot{y} = -b_1 y - b_2 z + b_3 x$	y	−1.5546	1.4611	0.1139	0.6076	0.7315
$\dot{z} = c_1(z - c_2)(x - c_3)$	z	1.6361	1.9200	0.0925	0.6168	0.7312
where $a_1 = 0.09$, $a_2 = 0.05$, $a_3 = 0.15$, $b - 1 = 0.06$, $b_2 = 0.085$, $b_3 = 0.07$, $b_4 = 0.07$, $c_1 = 0.1$, $c_2 = 0.041, 0.042$						
Flux controlled memristor [62]						
$\dot{x} = \frac{1}{C_1}[\frac{y-x}{R} - rx]$	x	−0.0145	3.7663	0.6712	0.8624	0.9455
$\dot{y} = \frac{1}{C_2}[\frac{x-y}{R} - z]$	y	−0.0000	0.3748	0.8951	0.8874	0.9883
$\dot{z} = \frac{y}{L}$	z	0.0017	0.2822	0.8733	0.8835	0.9959
$\dot{w} = -\frac{x}{\zeta}$	w	−0.0916	−1.8739	0.1006	0.3087	0.6974
where $\zeta = 8200 \times 47 \times 10^{-9}$; $R = 2000$; $C_1 = 6.8 \times 10^{-9}$; $C_2 = 68 \times 10^{-9}$; $L = 18 \times 10^{-3}$; $\alpha = -0.667 \times 10^{-3}$; $\beta = 0.029 \times 10^{-3}$; $r = -\alpha + 3\beta y^2$.						
Genesio and Tesi [63,64]						
$\dot{x} = y$	x	0.1377	−1.1867	0.6227	0.2463	0.9980
$\dot{y} = z$	y	0.3478	−1.2245	0.5156	0.1004	0.9931
$\dot{z} = -ax - by - cz + x^2$	z	0.1864	−1.1514	0.6580	0.2095	0.9697
where $a = 6$; $b = 2.92$; $c = 1.2$.						
Li et al. [65]						
$\dot{x} = -16x + 20yz$	x	−0.0051	−0.2485	0.7872	0.8415	0.8433
$\dot{y} = 10y - 6xz$	y	−0.0003	−0.6939	0.8603	0.7182	0.9157
$\dot{z} = -5z + 18y^2$	z	−0.0980	−0.9221	0.8613	0.7934	0.9360
Li and Sprott [66]						
$\dot{x} = yz$	x	0.0023	−0.2196	0.8567	0.9277	0.8624
$\dot{y} = 1 - z^2$	y	−0.2622	0.1621	0.9575	0.9152	0.9130
$\dot{z} = x + yz$	z	0.0094	0.3070	0.9607	0.5493	0.8597
Liu and Chen [67]						
$\dot{x} = 1.5x - yz$	x	0.0132	0.9226	0.9241	0.9580	0.7826
$\dot{y} = -10y + xz$	y	−0.0007	11.7760	0.3050	0.9763	0.5337
$\dot{z} = -4z + xy$	z	−0.0449	5.0172	0.5013	0.8873	0.7990
Lü and Chen [68]						
$\dot{x} = 36(y - x)$	x	−0.0002	−0.4949	0.9266	0.8457	0.8685
$\dot{y} = -xz + 20y$	y	−0.0006	−0.3236	0.9422	0.9108	0.8483
$\dot{z} = xy - 3z$	z	0.2535	−0.3539	0.9408	0.7114	0.9495
Lü et al. [69,70]						
$\dot{x} = 0.4x - yz$	x	0.0113	0.2948	0.9342	0.8041	0.5401
$\dot{y} = -12y + xz$	y	−0.1063	41.3350	0.0006	0.1884	0.0019
$\dot{z} = -5z + xy$	z	−0.0601	23.7057	0.0011	0.6488	0.0110
Memristive circuit [12,71]						
$\dot{x} = y$	x	−0.8235	0.0391	0.7455	0.6689	0.9496
$\dot{y} = -\frac{1}{3}[x + 1.52(z^2 - 1)y]$	y	0.4986	0.5598	0.8316	0.9146	0.8807
$\dot{z} = -y - 0.6z + yz$	z	−0.8277	−0.2585	0.6046	0.4188	0.9038
Özoğuz et al. [72]						
$\dot{x} = y$	x	0.0039	−0.8260	0.8818	0.8230	0.9784
$\dot{y} = z$	y	−0.0032	−0.6363	0.9356	0.7480	0.9489
$\dot{z} = -0.25(y + z) - af(x)$	z	−0.0048	−1.0010	0.8591	0.6947	0.9769
where $f(x) = \sum_{j=-3}^{5}(-1)^{j-1} \tanh k(x - 2j)$.						
Qi et al. [73]						
$\dot{x} = 14(y - x) + 4yz$	x	−0.0313	0.6421	0.9562	0.8812	0.9000
$\dot{y} = -x + 16y - xz$	y	0.0158	0.9269	0.9554	0.9238	0.9044
$\dot{z} = -43z + xy$	z	0.0375	4.1904	0.7527	0.8528	0.9239

Table A3. *Cont.*

Chaotic System	Output Variable	$\tilde{\mu}_3$	$\tilde{\mu}_4$	k_1	k_2	k_3
Ring oscillating systems [74]						
$\dot{x} = \alpha(Mf(z) - x)$	x	−0.0003	−0.7734	0.8992	0.7333	0.9900
$\dot{y} = 4\pi^2(x - z)$	y	0.0012	−0.5155	0.9619	0.9643	0.9762
$\dot{z} = y - \beta z$	z	0.0014	−1.1498	0.7992	0.7124	0.9259
where $\alpha = 2.1$; $\beta = 1.38$; $M = 5$; $f(z) = \lvert z+1\rvert - \lvert z-1\rvert + 0.5(\lvert z-4\rvert - \lvert z+4\rvert)$.						
Rössler [75]						
$\dot{x} = -y - z$	x	0.2261	−0.7120	0.8709	0.5620	0.9958
$\dot{y} = x + 0.2y$	y	−0.1768	−0.8174	0.8565	0.5895	0.9958
$\dot{z} = 0.2 + z(x - 6.5)$	z	5.3359	31.4457	0.0007	0.1869	0.4920
Sprott [76], system A						
$\dot{x} = y$	x	0.4457	0.1407	0.7233	0.8802	0.9472
$\dot{y} = -x + yz$	y	0.0004	0.6015	0.9336	0.8052	0.8718
$\dot{z} = 1 - y^2$	z	−0.0003	−0.7692	0.9357	0.5446	0.9792
Sprott [76], system B						
$\dot{x} = yz$	x	−0.0854	0.6461	0.9488	0.9882	0.8560
$\dot{y} = x - y$	y	−0.0859	−0.4976	0.9265	0.7967	0.9309
$\dot{z} = 1 - xy$	z	0.0550	1.0485	0.9573	0.9551	0.9124
Sprott [76], system C						
$\dot{x} = yz$	x	−0.0285	−0.1891	0.9670	0.9618	0.9479
$\dot{y} = x - y$	y	−0.0333	−0.9804	0.8582	0.8341	0.9715
$\dot{z} = 1 - x^2$	z	−0.6070	3.6133	0.8816	0.6143	0.9590
Sprott [76], system D, $[x_0, y_0, z_0] = [0.05, 0.05, 0.05]$						
$\dot{x} = -y$	x	−1.4687	1.7451	0.5122	0.9302	0.8719
$\dot{y} = x + z$	y	−0.2164	0.4422	0.8908	0.9015	0.9176
$\dot{z} = xz + 3y^2$	z	1.4479	1.8039	0.5215	0.8628	0.9014
Sprott [76], system E						
$\dot{x} = yz$	x	0.4423	0.7410	0.8625	0.6111	0.8678
$\dot{y} = x^2 - y$	y	7.8746	203.4464	0.2325	0.4360	0.8765
$\dot{z} = 1 - 4x$	z	−0.2077	−1.1366	0.7000	0.3984	0.9822
Sprott [76], system F, $[x_0, y_0, z_0] = [0.3196, 0.4268, 0.5159]$						
$\dot{x} = y + z$	x	−0.2414	−0.3601	0.9374	0.8712	0.9195
$\dot{y} = -x + 0.5y$	y	−0.7451	−0.4105	0.6865	0.8476	0.9080
$\dot{z} = x^2 - z$	z	1.5488	1.9861	0.3528	0.7115	0.8282
Sprott [76], system G, $[x_0, y_0, z_0] = [1.0755, 0.0291, 0.0274]$						
$\dot{x} = 0.4x + z$	x	−0.4155	−0.4738	0.7584	0.6293	0.8725
$\dot{y} = xz - y$	y	−1.3171	1.9318	0.5137	0.7544	0.8240
$\dot{z} = -x + y$	z	−0.2177	−0.4342	0.8068	0.8614	0.9355
Sprott [76], system H, $[x_0, y_0, z_0] = [0.9767, -0.6578, 0.1281]$						
$\dot{x} = -y + z^2$	x	−0.9067	1.0592	0.8259	0.8943	0.9268
$\dot{y} = x + 0.5y$	y	0.8846	0.1870	0.7236	0.8897	0.9088
$\dot{z} = x - z$	z	−0.2380	−0.3583	0.9374	0.8753	0.9163
Sprott [76], system I, $[x_0, y_0, z_0] = [0.05, 0.05, 0.05]$						
$\dot{x} = -0.2y$	x	−0.6289	−0.6397	0.5727	0.5888	0.9878
$\dot{y} = x + z$	y	−0.4225	−0.8321	0.7032	0.3328	0.9710
$\dot{z} = x + y^2 - z$	z	−0.1394	0.1985	0.7051	0.8696	0.8300
Sprott [76], system J						
$\dot{x} = -2z$	x	0.6591	−0.5538	0.6268	0.6359	0.9792
$\dot{y} = -2y + z$	y	−0.4453	−0.7307	0.7934	0.5190	0.9716
$\dot{z} = -x + y + y^2$	z	−0.7874	−0.2111	0.7026	0.5675	0.9482

Table A3. *Cont.*

Chaotic System	Output Variable	$\tilde{\mu}_3$	$\tilde{\mu}_4$	k_1	k_2	k_3
Sprott [76], system K						
$\dot{x} = xy - z$	x	−0.6564	−0.1459	0.8233	0.5426	0.9263
$\dot{y} = x - y$	y	−0.1882	−0.8507	0.8653	0.5430	0.9624
$\dot{z} = x + 0.3z$	z	0.9667	0.1361	0.5752	0.6775	0.9612
Sprott [76], system L, $[x_0, y_0, z_0] = [-7.3474, 30.4894, -5.4293]$						
$\dot{x} = y + 3.9z$	x	−0.4581	−1.0074	0.6298	0.2881	0.9741
$\dot{y} = 0.9x^2 - y$	y	0.6651	−0.4800	0.6865	0.7803	0.9235
$\dot{z} = 1 - x$	z	−0.4601	−0.4952	0.6950	0.6331	0.9728
Sprott [76], system M, $[x_0, y_0, z_0] = [-1.6768, -0.8718, 1.4698]$						
$\dot{x} = -z$	x	0.1887	−1.0776	0.6689	0.4527	0.9901
$\dot{y} = -x^2 - y$	y	−1.0221	0.2497	0.5754	0.7964	0.8224
$\dot{z} = 1.7 + 1.7x + y$	z	−0.6044	−0.7847	0.6011	0.2816	0.9553
Sprott [76], system N						
$\dot{x} = -2y$	x	−0.6613	−0.5537	0.6247	0.6483	0.9790
$\dot{y} = x_z^2$	y	−0.7877	−0.2074	0.7006	0.5577	0.9483
$\dot{z} = 1 + y - 2z$	z	−0.4452	−0.7278	0.7912	0.5151	0.9716
Sprott [76], system O, $[x_0, y_0, z_0] = [-0.4120, -0.5758, -0.7232]$						
$\dot{x} = y$	x	−0.1672	−0.9803	0.7362	0.4725	0.9929
$\dot{y} = x - z$	y	−0.3632	−1.1061	0.5690	0.2467	0.9963
$\dot{z} = x + xz + 2.7y$	z	−0.0199	−1.1439	0.7198	0.2928	0.9920
Sprott [76], system P, $[x_0, y_0, z_0] = [-0.0115, 0.5545, -0.2078]$						
$\dot{x} = 2.7y + z$	x	0.9197	0.1877	0.7137	0.9358	0.9261
$\dot{y} = -x + y^2$	y	−0.2534	−0.5963	0.8894	0.8862	0.9202
$\dot{z} = x + y$	z	0.7941	−0.1643	0.7097	0.8449	0.8992
Sprott [76], system Q						
$\dot{x} = -z$	x	−0.4461	−0.1058	0.8224	0.8859	0.9232
$\dot{y} = x - y$	y	−0.3738	−0.6333	0.7944	0.7859	0.9237
$\dot{z} = 3.1x + y^2 + 0.5z$	z	0.6820	0.1400	0.7650	0.8623	0.9857
Sprott [76], system R						
$\dot{x} = 0.9 - y$	x	−0.4423	−0.4140	0.8797	0.6456	0.9681
$\dot{y} = 0.4 + z$	y	0.8124	0.9527	0.8116	0.5035	0.8950
$\dot{z} = xy - z$	z	−1.9040	6.0313	0.4899	0.7703	0.6918
Sprott [76], system S						
$\dot{x} = -x - 4y$	x	−0.5469	−0.5727	0.7623	0.6349	0.9775
$\dot{y} = x + z^2$	y	0.5628	−0.4412	0.7384	0.8145	0.9541
$\dot{z} = 1 + x$	z	−0.4298	−0.7253	0.7986	0.7416	0.9527
Wu and Wang [77], $[x_0, y_0, z_0] = [0, 0, 0]$						
$0.2x + y$	x	−0.3147	−1.0386	0.7434	0.3887	0.9940
$-\frac{1}{3}(x - z^2 y)$	y	0.4113	−0.7459	0.8099	0.4452	0.9695
$-0.4y - 0.4z + yz$	z	−1.0675	0.0421	0.3894	0.6262	0.9119
Zhang et al. [78]						
$\dot{x} = y$	x	−0.0022	−0.4024	0.8803	0.7467	0.9745
$\dot{y} = -x - (-1 + z + 2z^2)y$	y	0.0166	−0.1566	0.9239	0.6519	0.9363
$\dot{z} = -2z + (0.5 + z + 2z^2)y^2$	z	1.8648	2.9939	0.2449	0.7947	0.8099

References

1. Moon, F.C. *Chaotic and Fractal Dynamics: Introduction for Applied Scientists and Engineers*; John Wiley & Sons: Hoboken, NJ, USA, 2008.
2. Kiel, L.D.; Elliott, E.W. *Chaos Theory in the Social Sciences: Foundations and Applications*; University of Michigan Press: Ann Arbor, MI, USA, 1997.
3. Turner, J.R.; Baker, R.M. Complexity Theory: An Overview with Potential Applications for the Social Sciences. *Systems* **2019**, *7*, 4. [CrossRef]
4. Scharf, Y. A chaotic outlook on biological systems. *Chaos Solitons Fractals* **2017**, *95*, 42–47. [CrossRef]

5. Fernández-Díaz, A. Overview and Perspectives of Chaos Theory and Its Applications in Economics. *Mathematics* **2023**, *12*, 92. [CrossRef]
6. Biswas, H.R.; Hasan, M.M.; Bala, S.K. Chaos theory and its applications in our real life. *Barishal Univ. J. Part* **2018**, *1*, 123–140.
7. Vasyuta, K.; Zots, F.; Zakharchenko, I. Building the air defense covert information and measuring system based on orthogonal chaotic signals. *Innov. Technol. Sci. Solut. Ind.* **2019**, *4*, 33–43. [CrossRef]
8. Macovei, C.; Răducanu, M.; Datcu, O. Image Encryption Algorithm Using Wavelet Packets and Multiple Chaotic Maps. In Proceedings of the 2020 International Symposium on Electronics and Telecommunications (ISETC), Timisoara, Romania, 5–6 November 2020; pp. 1–4. [CrossRef]
9. Kushnir, M.; Vovchuk, D.; Haliuk, S.; Ivaniuk, P.; Politanskyi, R. Approaches to Building a Chaotic Communication System. In *Data-Centric Business and Applications: ICT Systems-Theory, Radio-Electronics, Information Technologies and Cybersecurity*; Springer International Publishing: Cham, Switzerland, 2021; Volume 5, pp. 207–227. [CrossRef]
10. Kocarev, L.; Lian, S. *Chaos-Based Cryptography: Theory, Algorithms and Applications*; Springer Science & Business Media: Berlin/Heidelberg, Germany, 2011; Volume 354. [CrossRef]
11. Cang, S.; Kang, Z.; Wang, Z. Pseudo-random number generator based on a generalized conservative Sprott-A system. *Nonlinear Dyn.* **2021**, *104*, 827–844. [CrossRef]
12. Haliuk, S.; Krulikovskyi, O.; Vovchuk, D.; Corinto, F. Memristive Structure-Based Chaotic System for PRNG. *Symmetry* **2022**, *14*, 68. [CrossRef]
13. Kushnir, M.; Haliuk, S.; Rusyn, V.; Kosovan, H.; Vovchuk, D. Computer Modeling of Information Properties of Deterministic Chaos. In Proceedings of the CHAOS 2014—Proceedings: 7th Chaotic Modeling and Simulation International Conference, Lisbon, Portugal, 7–10 June 2014; pp. 265–276.
14. Kushnir, M.; Ivaniuk, P.; Vovchuk, D.; Galiuk, S. Information Security of the Chaotic Communication Systems. In Proceedings of the CHAOS 2015—8th Chaotic Modeling and Simulation International Conference, Paris, France, 26–29 May 2015; pp. 441–452.
15. Wang, Y.; Liu, Z.; Zhang, L.Y.; Pareschi, F.; Setti, G.; Chen, G. From chaos to pseudorandomness: A case study on the 2-D coupled map lattice. *IEEE Trans. Cybern.* **2023**, *53*, 1324–1334. [CrossRef] [PubMed]
16. Cover, T.; Thomas, J.A. *Elements of Information Theory*; Wiley-Interscience: Hoboken, NJ, USA, 2006.
17. Eisencraft, M.; Monteiro, L.H.A.; Soriano, D.C. White Gaussian Chaos. *IEEE Commun. Lett.* **2017**, *21*, 1719–1722. [CrossRef]
18. Mliki, E.; Hasanzadeh, N.; Nazarimehr, F.; Akgul, A.; Boubaker, O.; Jafari, S. Some New Chaotic Maps With Application in Stochastic. In *Recent Advances in Chaotic Systems and Synchronization*; Boubaker, O., Jafari, S., Eds.; Emerging Methodologies and Applications in Modelling; Academic Press: Cambridge, MA, USA, 2019; pp. 165–185. [CrossRef]
19. Rovatti, R.; Setti, G.; Callegari, S. Limit properties of folded sums of chaotic trajectories. *IEEE Trans. Circuits Syst. Fundam. Theory Appl.* **2002**, *49*, 1736–1744. [CrossRef]
20. Kilias, T.; Kelber, K.; Mogel, A.; Schwarz, W. Electronic chaos generators—Design and applications. *Int. J. Electron.* **1995**, *79*, 737–753. [CrossRef]
21. Liu, J.D.; Kai, Y.; Wang, S.H. Coupled Chaotic Tent Map Lattices System with Uniform Distribution. In Proceedings of the 2010 2nd International Conference on E-Business and Information System Security, Wuhan, China, 22–23 May 2010; pp. 1–5. [CrossRef]
22. Li, P.; Li, Z.; Halang, W.A.; Chen, G. A stream cipher based on a spatiotemporal chaotic system. *Chaos Solitons Fractals* **2007**, *32*, 1867–1876. [CrossRef]
23. Espinel, A.; Taralova, I.; Lozi, R. New alternate ring-coupled map for multi-random number generation. *J. Nonlinear Syst. Appl.* **2013**, *4*, 64–69.
24. Haliuk, S.; Krulikovskyi, O.; Politanskyi, L. Analysis of time series generated by Tratas chaotic system. *Her. Khmelnytskyi Natl. Univ.* **2017**, *251*, 187–192.
25. Haliuk, S.; Krulikovskyi, O.; Politanskyi, L.; Corinto, F. Circuit implementation of Lozi ring-coupled map. In Proceedings of the 2017 4th International Scientific-Practical Conference Problems of Infocommunications, Kharkov, Ukraine, 10–13 October 2017; Science and Technology (PIC S&T); IEEE: Piscataway, NJ, USA, 2017; pp. 249–252. [CrossRef]
26. Naruse, M.; Kim, S.J.; Aono, M.; Hori, H.; Ohtsu, M. Chaotic oscillation and random-number generation based on nanoscale optical-energy transfer. *Sci. Rep.* **2014**, *4*, 6039. [CrossRef] [PubMed]
27. Elsonbaty, A.; Hegazy, S.F.; Obayya, S.S.A. Numerical analysis of ultrafast physical random number generator using dual-channel optical chaos. *Opt. Eng.* **2016**, *55*, 094105. [CrossRef]
28. Yoshiya, K.; Terashima, Y.; Kanno, K.; Uchida, A. Entropy evaluation of white chaos generated by optical heterodyne for certifying physical random number generators. *Opt. Express* **2020**, *28*, 3686–3698. [CrossRef] [PubMed]
29. Kawaguchi, Y.; Okuma, T.; Kanno, K.; Uchida, A. Entropy rate of chaos in an optically injected semiconductor laser for physical random number generation. *Opt. Express* **2021**, *29*, 2442–2457. [CrossRef] [PubMed]
30. Baby, H.T.; Sujatha, B.R. Optical Chaos KEY generator for Cryptosystems. *J. Phys. Conf. Ser.* **2021**, *1767*, 012046. [CrossRef]
31. Nguyen, N.; Kaddoum, G.; Pareschi, F.; Rovatti, R.; Setti, G. A fully CMOS true random number generator based on hidden attractor hyperchaotic system. *Nonlinear Dyn.* **2020**, *102*, 2887–2904. [CrossRef]
32. Guo, Y.; Li, H.; Wang, Y.; Meng, X.; Zhao, T.; Guo, X. Chaos with Gaussian invariant distribution by quantum-noise random phase feedback. *Opt. Express* **2023**, *19*, 31522–31532. [CrossRef]

33. Fadil, E.; Abass, A.; Tahhan, S. Secure WDM-free space optical communication system based optical chaotic. *Opt. Quantum Electron.* **2022**, *54*, 477. [CrossRef]
34. Wang, L.; Mao, X.; Wang, A.; Wang, Y.; Gao, Z.; Li, S.; Yan, L. Scheme of coherent optical chaos communication. *Opt. Lett.* **2020**, *45*, 4762–4765. [CrossRef] [PubMed]
35. Liu, B.C.; Xie, Y.Y.; Zhang, Y.S.; Ye, Y.C.; Song, T.T.; Liao, X.F.; Liu, Y. ARM-Embedded Implementation of a Novel Color Image Encryption and Transmission System Based on Optical Chaos. *IEEE Photonics J.* **2020**, *12*, 1–17. [CrossRef]
36. Shakeel, I.; Hilliard, J.; Zhang, W.; Rice, M. Gaussian-Distributed Spread-Spectrum for Covert Communications. *Sensors* **2023**, *23*, 4081. [CrossRef] [PubMed]
37. Negi, R.; Goel, S. Secret Communication Using Artificial Noise. In Proceedings of the VTC-2005-Fall. 2005 IEEE 62nd Vehicular Technology Conference, Dallas, TX, USA, 28 September 2005; Volume 3, pp. 1906–1910. [CrossRef]
38. Zhou, X.; McKay, M.R. Secure Transmission with Artificial Noise Over Fading Channels: Achievable Rate and Optimal Power Allocation. *IEEE Trans. Veh. Technol.* **2010**, *59*, 3831–3842. [CrossRef]
39. Nguyen, L.L.; Nguyen, T.T.; Fiche, A.; Gautier, R.; Ta, H.Q. Hiding Messages in Secure Connection Transmissions with Full-Duplex Overt Receiver. *Sensors* **2022**, *22*, 5812. [CrossRef] [PubMed]
40. Yang, W.; Lu, X.; Yan, S.; Shu, F.; Li, Z. Age of Information for Short-Packet Covert Communication. *IEEE Wirel. Commun. Lett.* **2021**, *10*, 1890–1894. [CrossRef]
41. Anderson, D.F.; Seppäläinen, T.; Valkó, B. *Introduction to Probability*; Cambridge University Press: Cambridge, UK, 2017.
42. Athreya, K.B.; Lahiri, S.N. *Measure Theory and Probability Theory*; Springer: Berlin/Heidelberg, Germany, 2006; Volume 19.
43. Thode, H.C. *Testing for Normality*, 1st ed.; Statistics: Textbooks and Monographs 164; Marcel Dekker: New York, NY, USA, 2002.
44. Michalowicz, J.V.; Nichols, J.M.; Bucholtz, F. *Handbook of Differential Entropy*; CRC Press: Boca Raton, FL, USA, 2013.
45. Krasil'nikov, A.I. Class of non-Gaussian distributions with zero skewness and kurtosis. *Radioelectron. Commun. Syst.* **2013**, *56*, 312–320. [CrossRef]
46. Kschischang, F.R. *The Hilbert Transform*; University of Toronto: Toronto, ON, Canada, 2006.
47. Shannon, C.E. A mathematical theory of communication. *Bell Syst. Tech. J.* **1948**, *27*, 379–423. [CrossRef]
48. Kullback, S.; Leibler, R.A. On information and sufficiency. *Ann. Math. Stat.* **1951**, *22*, 79–86. [CrossRef]
49. Matsumoto, T.; Chua, L.; Komuro, M. The double scroll. *IEEE Trans. Circuits Syst.* **1985**, *32*, 797–818. [CrossRef]
50. Zhong, G.Q. Implementation of Chua's circuit with a cubic nonlinearity. *IEEE Trans. Circuits Syst. Fundam. Theory Appl.* **1994**, *41*, 934–941. [CrossRef]
51. Shi, Z.; Ran, L. Tunnel Diode Based Chua's Circuit. In Proceedings of the IEEE 6th Circuits and Systems Symposium on Emerging Technologies: Frontiers of Mobile and Wireless Communication (IEEE Cat. No.04EX710), 31 May–2 June 2004; Volume 1, pp. 217–220. [CrossRef]
52. Kennedy, M.P. Robust op amp realization of Chua's circuit. *Frequenz* **1992**, *46*, 66–80. [CrossRef]
53. Lorenz, E.N. Deterministic nonperiodic flow. *J. Atmos. Sci.* **1963**, *20*, 130–141. [CrossRef]
54. Pappu, C.S.; Flores, B.C.; Debroux, P.S.; Boehm, J.E. An Electronic Implementation of Lorenz Chaotic Oscillator Synchronization for Bistatic Radar Applications. *IEEE Trans. Aerosp. Electron. Syst.* **2017**, *53*, 2001–2013. [CrossRef]
55. Horowitz, P. *Build a Lorenz Attractor*; Harvard University: Cambridge, MA, USA, 2003.
56. Bhalekar, S.; Daftardar-Gejji, V. A New Chaotic Dynamical System and Its Synchronization. In Proceedings of the International Conference on Mathematical Sciences in Honor of Prof. AM Mathai, Palai, India, 3–5 January 2011; pp. 3–5.
57. Chen, H.K.; Lee, C.I. Anti-control of chaos in rigid body motion. *Chaos Solitons Fractals* **2004**, *21*, 957–965. [CrossRef]
58. Cheng, G.; Li, D.; Yao, Y.; Gui, R. Multi-scroll chaotic attractors with multi-wing via oscillatory potential wells. *Chaos Solitons Fractals* **2023**, *174*, 113837. [CrossRef]
59. Dmitriev, A.; Panas, A. *Dynamic Chaos: New Data Carrying Media for Communication Systems*; Fismatlit: Moscow, Russia, 2002. (In Russian)
60. Semenov, A. Reviewing the Mathemetical Models and Electrical Circuits of Deterministic Chaos Transistor Oscillators. In Proceedings of the 2016 International Siberian Conference on Control and Communications (SIBCON), Moscow, Russia, 12–14 May 2016; pp. 1–6. [CrossRef]
61. Dong, G.; Du, R.; Tian, L.; Jia, Q. A novel 3D autonomous system with different multilayer chaotic attractors. *Phys. Lett. A* **2009**, *373*, 3838–3845. [CrossRef]
62. Muthuswamy, B. Implementing memristor based chaotic circuits. *Int. J. Bifurc. Chaos* **2010**, *20*, 1335–1350. [CrossRef]
63. Genesio, R.; Tesi, A. Harmonic balance methods for the analysis of chaotic dynamics in nonlinear systems. *Automatica* **1992**, *28*, 531–548. [CrossRef]
64. Park, J.H. Synchronization of Genesio chaotic system via backstepping approach. *Chaos Solitons Fractals* **2006**, *27*, 1369–1375. [CrossRef]
65. Li, C.; Li, H.; Tong, Y. Analysis of a novel three-dimensional chaotic system. *Optik* **2013**, *124*, 1516–1522. [CrossRef]
66. Li, C.; Sprott, J.C. Variable-boostable chaotic flows. *Optik* **2016**, *127*, 10389–10398. [CrossRef]
67. Liu, W.; Chen, G. A new chaotic system and its generation. *Int. J. Bifurc. Chaos* **2003**, *13*, 261–267. [CrossRef]
68. LÜ, J.; Chen, G. A new chaotic attractor coined. *Int. J. Bifurc. Chaos* **2002**, *12*, 659–661. [CrossRef]
69. Lü, J.; Chen, G.; Cheng, D. A new chaotic system and beyond: The generalized lorenz-like system. *Int. J. Bifurc. Chaos* **2004**, *14*, 1507–1537. [CrossRef]

70. Huang, J.; Xiao, T.J. Chaos synchronizations of chaotic systems via active nonlinear control. *J. Phys. Conf. Ser.* **2008**, *96*, 012177. [CrossRef]
71. Muthuswamy, B.; Chua, L.O. Simplest chaotic circuit. *Int. J. Bifurc. Chaos* **2010**, *20*, 1567–1580. [CrossRef]
72. Özoguz, S.; Elwakil, A.; Salama, K.N. N-scroll chaos generator using nonlinear transconductor. *Electron. Lett.* **2002**, *38*, 1. [CrossRef]
73. Qi, G.; Chen, G.; van Wyk, M.A.; van Wyk, B.J.; Zhang, Y. A four-wing chaotic attractor generated from a new 3-D quadratic autonomous system. *Chaos Solitons Fractals* **2008**, *38*, 705–721. [CrossRef]
74. Haliuk, S.; Kushnir, M.; Politanskyi, L.; Politanskyi, R. Synchronization of chaotic systems and signal filtration in the communication channel. *East.-Eur. J. Enterp. Technol.* **2012**, *1*, 20–24. [CrossRef]
75. Rössler, O.E. An equation for continuous chaos. *Phys. Lett. A* **1976**, *57*, 397–398. [CrossRef]
76. Sprott, J.C. Some simple chaotic flows. *Phys. Rev. E* **1994**, *50*, R647. [CrossRef] [PubMed]
77. Wu, R.; Wang, C. A New Simple Chaotic Circuit Based on Memristor. *Int. J. Bifurc. Chaos* **2016**, *26*, 1650145. [CrossRef]
78. Zhang, X.; Tian, Z.; Li, J.; Cui, Z. A Simple Parallel Chaotic Circuit Based on Memristor. *Entropy* **2021**, *23*, 719. [CrossRef]